NJC

PAPER

View Article Online
View Journal | View Issue

Cite this: *New J. Chem.*, 2025, **49**, 5694

Unlocking MOF A520 synthesis: investigating critical parameters†

Marie Froehly,[ab] Gérald Chaplais,[b]* Habiba Nouali,[b] Vincent Roucoules[b] and T. Jean Daou[a]*

Received 6th February 2025,
Accepted 21st February 2025

DOI: 10.1039/d5nj00496a

rsc.li/njc

Aluminium based metal–organic frameworks (MOFs) have emerged as versatile materials with applications in gas and vapor storage, catalysis, and separation. Among these, aluminium fumarate known as MOF A520 or MIL-53(Al)_Fu exhibits promising humidity scavenging properties due to its unique structure, chemical composition and porosity. However, achieving reproducible, low cost and high-yield synthesis remains a challenge. In this study, we systematically investigate the critical parameters influencing green synthesis of MOF A520. Through a hydrothermal method, we explore the impact of aluminium precursor nature and concentration, water and base concentrations in the starting mixture and reaction time. Our findings reveal optimal conditions for MOF A520 crystallization, leading to enhanced yield, purity and cost reduction. This work bridges the gap between laboratory-scale synthesis and industrial-scale production, providing insights that are not available in existing literature.

Introduction

Aluminium fumarate is a hydrophilic MOF displaying a crystal structure with the same bpq topology as that of the well-known MIL-53(Al).[1] Indeed, aluminium fumarate, with the formula {Al(OH)(O_2C–CH=CH–CO_2)}, is made up of infinite Al–OH–Al chains linked by fumarate linkers, generating a 1D porous network consisting of lozenge channels with a pore diameter of 5.7 × 6.0 Å^2.[1]

Aluminium fumarate has been used in many applications, in powder or shaped forms: as a scavenger for molecular decontamination in a vapor or gas phase (water,[2–8] CO_2,[2,9] N_2,[2] NH_3[10] and dichloromethane[11]); for heat transformation applications;[12–22] to remove pollutants from water such as fluoride[23,24] and phosphate;[25] for methane purification;[26–28] to improve the hydrophilicity of poly(ether-sulfone) membranes;[29] as an anode for lithium-ion batteries[30] and as a derived support for hydrogen production from methanol steam reforming.[31]

Thanks to its numerous applications, attention was paid to optimizing the synthesis of aluminium fumarate in order to facilitate its industrialization, such as continuous flow synthesis[32] or synthesis by extrusion under solvent-free conditions.[33,34] This MOF has even been marketed for a time by BASF as Basolite™ A520 from a hydrothermal synthesis using aluminium sulfate as the aluminium precursor.[35] Thus, the usual protocol for synthesizing MOF A520 consists of a reaction under stoichiometric conditions between aluminium sulfate octadecahydrate and fumaric acid in water for 2 h at 60 °C. Two molar equivalents of NaOH are added for the linker deprotonation in water.[24] Besides $Al_2(SO_4)_3{\cdot}18H_2O$, a commonly used precursor,[1,3,6,7,12,17,19,23,24,26,29,30,32] other sources of aluminium, needed to synthesize MOF A520, such as $AlCl_3{\cdot}6H_2O$[3,4,16,30] and $Al(NO_3)_3{\cdot}9H_2O$,[3,9,30] have been used, without significant variation in the properties of the obtained MOF A520. However, these aluminium salts are relatively expensive (around a hundred euros per kilo), resulting in an expensive final product. Other less expensive sources of aluminium are therefore necessary to prepare the MOF A520 and market it at a more attractive price. Thus, a cheaper reagent, sodium aluminate, has been successfully studied for the synthesis of MOF A520 but an excess of fumaric acid (molar ratio: 1 $NaAlO_2$/1.7 fumaric acid) needs to be used to counterbalance the basic pH imposed by the presence of this precursor.[11,28] Aluminium hydroxide could be an interesting alternative to sodium aluminate, with a similar price but lower basicity. In this way, this study first aims to perform the synthesis of MOF A520 from inexpensive reagents, such as aluminium hydroxide and sodium aluminate but under stoichiometric conditions, in order to minimize reagent losses and therefore the synthesis cost.

Moreover, MOF A520 crystals commonly obtained from aluminium sulfate octadecahydrate are highly agglomerated and nanometer-sized with a crystallite size distribution between 60 and 100 nm.[17] Thus, this makes their collection difficult on an industrial scale. Nevertheless, other particle

[a] *APTAR CSP Technologies, F-67110 Niederbronn-les-Bains, France. E-mail: jean.daou@aptar.com*
[b] *Université de Haute-Alsace (UHA), Université de Strasbourg (UniStra), CNRS, Institut de Science des Matériaux de Mulhouse (IS2M), UMR 7361, Axe Matériaux à Porosité Contrôlée (MPC), F-68100 Mulhouse, France. E-mail: gerald.chaplais@uha.fr*

† Electronic supplementary information (ESI) available. See DOI: https://doi.org/10.1039/d5nj00496a

sizes can be obtained depending on the protocol used. For example, by replacing NaOH with urea ($CO(NH_2)_2$) for the linker deprotonation, Alvarez *et al.* obtained flat crystals of approximately 400 nm agglomerated into a sphere of approximately 4.6 μm by heating for 15 min at 130 °C in a microwave oven.[1] According to Han *et al.*, the solvothermal synthesis of MOF A520 in DMF from aluminium chloride hexahydrate, stirred for 4 days at 130 °C, allows the formation of crystals from 500 nm to 1 μm.[4] Finally, Li *et al.* used an alternative way by altering the common molar NaOH/Al source fixed to 2 by a low ratio molar KOH/Al source (0.1) and then incubating the solution for 12 h at 100 °C. This leads to the formation of 500 nm to 1.5 μm sized needle crystals of MOF A520.[19] This last protocol, described by Li *et al.*, has the advantage of being able to be carried out in an oven without an organic solvent, unlike the two other processes described above. In this way, to grow the crystals in order to facilitate the collection and industrial production of MOF A520, the influence of the base nature (NaOH or KOH) and its molar ratio (from 0.1 to 2) has been studied.

In this paper, we delve into the intricacies of MOF A520 hydrothermal green synthesis, systematically exploring parameters such as aluminium precursors, base natures and ratios, and reaction conditions. A special focus is made on the humidity scavenging properties of the obtained MOF A520 for future applications in pharmaceutical packaging to increase the shelf life of humidity sensitive drugs. Indeed, water present in the atmosphere (moisture), often expressed in terms of relative humidity, is an essential parameter to be monitored for many industrials since it can be a major source of contamination affecting the global performances of several applications.[36,37] These detrimental effects are also observed when it comes to the purity of chemicals,[38] on the efficiency of medical devices[39] or also regarding the packaging of active components for drugs.[40,41] Several adsorbents can be used to overcome the presence of moisture: anhydrous salts,[38] clays,[42] activated carbon,[43] silica gel,[42,44] metal–organic frameworks (MOFs)[45] and aluminosilicate zeolites, especially 3A or 4A zeolites which are widely used on an industrial scale.[42,46,47] MOF A520 synthesized with both green and low cost methods can be an alternative for 3A and 4A zeolites due its higher water adsorption capacity ranging between 44 and 47 wt% (at an 80% relative humidity (RH))[13,17] compared to 3A and 4A zeolites ranging between 21 and 25 wt%.[48] Thus, the main objective of this article is to determine the synthesis parameter(s) significantly influencing the properties of the synthesized MOF A520, in order to propose an optimized protocol to facilitate its future industrial production at a reduced cost.

Materials and methods

Material synthesis

Reactants, bases, acids and solvents. Aluminium sulfate octadecahydrate ($Al_2(SO_4)_3{\cdot}18H_2O$, CAS-No. 7784-31-8, Sigma-Aldrich, 97%), sodium aluminate ($NaAlO_2$, CAS-No. 11138-49-1, Sigma-Aldrich, 83%), aluminium hydroxide ($Al(OH)_3$ (gibbsite), CAS-No. 21645-51-2, Alumina, 99%), fumaric acid ($C_4H_4O_4$, CAS-No. 110-17-8, Sigma-Aldrich, 99%), sodium hydroxide (NaOH, CAS-No. 1310-73-2, Sigma-Aldrich, 98%), potassium hydroxide (KOH, CAS-No. 1310-58-3, Sigma-Aldrich, 85%), sulfuric acid (H_2SO_4, CAS-No. 7664-93-9, Sigma-Aldrich, 96%) and hydrochloric acid (HCl, CAS-No. 7647-01-0, Carlo Erba, 37%) were used as purchased without further purification and demineralized water (DI) was produced in house by exchange on resin (18 MΩ cm).

Protocols. The different samples of MOF A520 were synthesized by a hydrothermal method following modified procedures described by Karmakar *et al.*,[24] Wamba *et al.*,[28] and Li *et al.*[19] The description of these protocols is given in the following paragraphs.

Synthesis of MOF A520 from aluminium hydroxide (protocol 1). For the synthesis of MOF A520 from aluminium hydroxide according to protocol 1, the molar ratios, the reflux duration and the pH of the reaction medium are reported in Table 1. The required amount of NaOH, 6 g (150 mmol) for sample 1; 2 g (50 mmol) for sample 2; 4 g (100 mmol) for sample 3 and 6 g (150 mmol) for sample 4, is dissolved in 45 g (2498 mmol) of DI water in a 250 mL glass flask under stirring (250 rpm) topped with an air condenser. The solution is heated at 100 °C before adding 4 g (51 mmol) of $Al(OH)_3$ (solution S1). The mixture is heated, stirred and maintained for the time given in Table 1. Meanwhile, in a 500 mL polypropylene (PP) bottle, 5.9 g (51 mmol) of fumaric acid are dissolved in 115 g (6383 mmol) of water at 95 °C (solution S2). After dissolution, solution S1 is poured quickly and at once into solution S2. For sample 4, 7.8 g (80 mmol) of H_2SO_4 are added dropwise with a Pasteur pipette to lower the solution pH to 3. After homogenization, the bottle (with a solution for sample 1 and a suspension for others) is closed and placed for 2 hours in an oven preheated to 65 °C. After cooling to room temperature for 30 min, the mixture is centrifuged in two 250 mL PP tubes for 5 min at 8500 rpm. The supernatant is removed. The white powder is then washed several times by dispersion into 2 tubes with approximately 140 mL of DI water per tube and 5 min of ultrasound treatment. The washing step is repeated (1 washing for samples 2 and 3,

Table 1 Experimental conditions for MOF A520 synthesis from aluminium hydroxide according to protocol 1: molar ratios, reflux duration and pH

	$Al(OH)_3$	$C_4H_4O_4$	NaOH	H_2SO_4	H_2O	Reflux duration (hours)	pH[a] S1 + S2	pH[b] S1 + S2 + H_2SO_4
Sample 1	1	1	3	—	175	1	14	—
Sample 2	1	1	1	—	175	3.5	3.5	—
Sample 3	1	1	2	—	175	2.5	6	—
Sample 4	1	1	3	1.6	175	1	14	3

[a] pH measurements after mixing the two solutions S1 ($Al(OH)_3$ + NaOH + H_2O) and S2 ($C_4H_4O_4$ + H_2O) were performed with pH indicator rods. [b] pH measurements after adding sulfuric acid were performed with pH indicator rods.

Table 2 Experimental conditions for MOF A520 synthesis from sodium aluminate according to protocol 2: molar ratios and pH

	$NaAlO_2$	$C_4H_4O_4$	Acid	H_2O	pH[a]	pH[b] after acid addition
Sample 5	1	1	—	175	6	—
Sample 6	1	1	0.7 H_2SO_4	175	6	3
Sample 7	1	1	1.2 HCl	179	6	3

[a] pH measurements after mixing the aluminium source and the linker in water ($NaAlO_2$ + $C_4H_4O_4$ + H_2O) were performed with pH indicator rods. [b] pH measurements after adding sulfuric acid or hydrochloric acid were performed with pH indicator rods.

and 4 washings for samples 1 and 4) until the supernatant displays a pH of 4.5–6. Finally, the white powder is dried overnight in an oven at 90 °C (1.1 g for sample 1; 4.7 g for sample 2; 3.4 g for sample 3 and 4.2 g for sample 4).

Synthesis of MOF A520 from sodium aluminate (protocol 2). In the case of the synthesis of MOF A520 from sodium aluminate according to protocol 2, the molar ratios and the pH of the reaction medium are reported in Table 2. 700 g (38 856 mmol) of DI water are pre-heated in a 1 L PP bottle at 65 °C inside an oven for 24 h. Then, 22 g (222 mmol) of $NaAlO_2$ are added and fully dissolved with stirring (250 rpm). Then, 25.80 g (222 mmol) of fumaric acid are added.

For sample 6, 15 g (153 mmol) of H_2SO_4 are added dropwise with a Pasteur pipette. For sample 7, 26.2 g (266 mmol) of HCl are added dropwise with a Pasteur pipette. Acid is added to these two samples to lower the solution pH to 3. After homogenization, the bottle is closed and placed for 2 h in an oven preheated to 65 °C. After cooling to room temperature for 30 min, the mixture is centrifuged in six 250 mL PP tubes for 5 min at 8500 rpm. The supernatant is removed. The white gel is then washed several times by dispersion into 6 tubes with approximately 120 mL of DI water per tube and 5 min of ultrasound treatment. The washing step is repeated (1 washing for sample 5, 5 washings for sample 6, and 6 washings for sample 7) until the supernatant displays a pH of 4.5–6. After drying overnight in an oven at 90 °C, the white agglomerated powder is manually ground. Finally, the white powder is heated for 24 h at 150 °C in an oven.

Synthesis of MOF A520 from aluminium sulfate octadecahydrate using two type of bases (protocol 3). The synthesis conditions for the synthesis of MOF A520 from aluminium sulfate octadecahydrate with two types of bases commonly used for the linker deprotonation in water, KOH or NaOH are summarized in Table 3. The synthetic procedure is given in protocols 3(a) and (b) according to Li *et al.*[19] and Karmakar *et al.*,[24] respectively. The main differences between these two protocols are the temperature, the synthesis duration and the water molar ratio.

(a) The required amount of NaOH (0.4 g, 9 mmol, for sample 10) or KOH (0.6 g, 9 mmol for samples 8 and 9; 2.7 g, 41 mmol for sample 11; 4.3 g, 65 mmol for samples 12, 13 and 14; 5.3 g, 80 mmol for sample 15 and 10.6 g, 160 mmol for sample 16) is dissolved in 100 g (5551 mmol) of DI water in a 500 mL PP bottle. 26.70 g (40 mmol) of $Al_2(SO_4)_3{\cdot}18H_2O$ and 9.30 g (80 mmol) of fumaric acid are added to the basic solution with stirring (250 rpm). The closed bottle is placed in an oven preheated to 100 °C and left for the duration defined in Table 3. After cooling to room temperature for 1 h, the white gel is recovered either by filtration on Büchner (Whatman no. 5 filter paper) or by centrifugation (6 PP tubes of 250 mL, 8500 rpm for 5 min), and then washed several times with approximately 500 mL of DI water and 5 min of ultrasound. The washing step is repeated 5 times until a pH of the supernatant/filtrate is greater than 4.5. After drying overnight in an oven at 90 °C, the white agglomerated powder is manually ground. Finally, the white powder is heated for 24 h at 150 °C in an oven.

(b) 700 g (38 856 mmol) of DI water is heated in an oven at 65 °C for 24 hours before synthesis. 74.20 g (111 mmol) of $Al_2(SO_4)_3{\cdot}18H_2O$ are dissolved in 318 g (17 652 mmol) of hot water in a 1 L PP bottle with stirring (250 rpm) (solution S1). In another 1 L PP bottle with stirring (250 rpm), 25.80 g (222 mmol) of fumaric acid and the required amount of KOH (31.4 g, 475 mmol for sample 17) or NaOH (19.0 g, 475 mmol for sample 18) are dissolved in 382 g (21 204 mmol) of hot water (solution S2). After dissolution, solution S2 is poured quickly and at once into solution S1. After homogenization, the closed bottle is placed for 2 hours at 65 °C in an oven. After cooling to room temperature during 1 h, the mixture is centrifuged in six 250 mL PP tubes for 5 min at 8500 rpm. The supernatant is removed. The white gel is then washed several times by

Table 3 Experimental conditions for MOF A520 synthesis from aluminium sulfate octadecahydrate according to protocols 3: molar ratios, duration, temperature and pH

	$Al_2(SO_4)_3{\cdot}18H_2O$	$C_4H_4O_4$	Base	H_2O	Protocol	Duration	Temperature (°C)	pH[a]
Sample 8	1	1	0.1 KOH	78	(a)	13 h 30	100	1
Sample 9	1	1	0.1 KOH	78	(a)	42 h 30	100	1
Sample 10	1	1	0.1 NaOH	78	(a)	44 h 15	100	1
Sample 11	1	1	0.5 KOH	78	(a)	14 h 30	100	1
Sample 12	1	1	0.8 KOH	78	(a)	15 h 15	100	1
Sample 13	1	1	0.8 KOH	78	(a)	42 h 30	100	1
Sample 14	1	1	0.8 KOH	78	(a)	71 h 30	100	1
Sample 15	1	1	1 KOH	78	(a)	13 h 20	100	1
Sample 16	1	1	2 KOH	78	(a)	13 h 20	100	2.5–3
Sample 17	1	1	2 KOH	184	(b)	2 h	65	2.5–3
Sample 18	1	1	2 NaOH	184	(b)	2 h	65	2.5–3

[a] pH measurements after mixing all reagents ($Al_2(SO_4)_2{\cdot}18H_2O$ + $C_4H_4O_4$ + KOH or NaOH + H_2O) were performed with pH indicator rods.

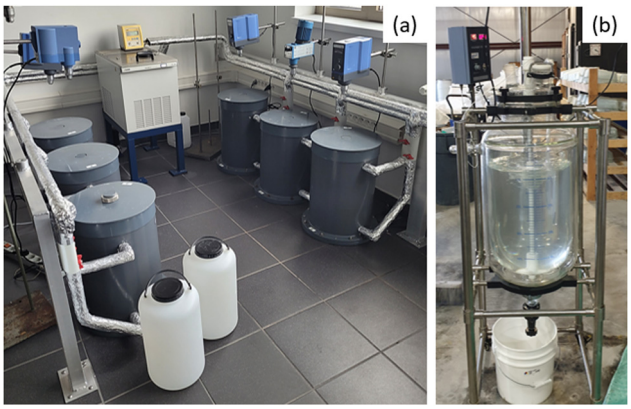

Fig. 1 (a) Heating station and 10 L PP bottles used for the scale up ×10. (b) The 100 L glass reactor used for the ×100 scale up.

dispersion in the 6 tubes with approximately 120 mL of DI water per tube and 5 min of ultrasound treatment. The washing step is repeated 5 times until a pH of the supernatant greater than 4.5 is reached. After drying overnight in an oven at 90 °C, the white agglomerated powder is manually ground. Finally, the white powder is heated for 24 h at 150 °C in an oven.

Scale-ups of the MOF A520 synthesis from aluminium sulfate octadecahydrate (protocol 4). We carried out a scale-up of MOF A520 from the protocol known in the literature in order to check its reproducibility on a large scale. Two scaled-up syntheses were performed based on protocol 3(b). The first one with a factor of 10 was performed in 10 L PP bottles and repeated 10 times. The second one with a factor of 100 was performed in 100 L glass reactors (Fig. 1). For all syntheses following this protocol 4, the molar ratios applied are 1 $Al_2(SO_4)_3{\cdot}18H_2O$: 1 $C_4H_4O_4$: 2 NaOH : 184 H_2O.

For the 10-factor scaled-up preparation, 3190 g (177 mol) (bottle 1) and 3820 g (212 mol) (bottle 2) of DI water are pre-heated with a heating station (hot oil circulation) at 60 °C for 4 hours before synthesis. Then, 742 g (1.1 mol) of $Al_2(SO_4)_3{\cdot}18H_2O$ are dissolved in bottle 1 under stirring (300 rpm) and 247 g (2.1 mol) of fumaric acid and 192 g (4.8 mol) of NaOH are dissolved in bottle 2 under stirring (300 rpm). After dissolution, the solution of bottle 2 is poured quickly and at once into bottle 1. The white suspension is heated for 2 hours at 60 °C with 300 rpm stirring. After cooling to room temperature, the mixture is centrifuged for 5 min at 8500 rpm. The supernatant is removed after the pH measurement with pH indicator rods (pH = 2.5–3). The white gel is then washed several times by dispersion in two 5 L beakers with each 3 L of DI water and 10 min of ultrasound treatment. The washing step is repeated 4 times until a pH of the supernatant greater than 4.5 is reached. After drying overnight in an oven at 90 °C, the white agglomerated powder is manually ground. Finally, the white powder is heated for 24 h at 100 °C in a vacuum oven.

For the 100-factor scaled-up synthesis, in reactor 1, 7.4 kg (11 mol) of $Al_2(SO_4)_3{\cdot}18H_2O$ are dissolved in 32 kg (1776 mol) of DI water with stirring (240 rpm) and heated with a heating mantle at 60 °C. In reactor 2, 2.5 kg (22 mol) of fumaric acid and 1.9 kg (48 mol) of NaOH are dissolved in 38 kg (2109 mol) of DI water with stirring (240 rpm). After dissolution, the solution of reactor 2 is poured into reactor 1. The white suspension is heated for 2 hours at 60 °C with 240 rpm stirring. After cooling to room temperature, the mixture is collected with a spin dryer at 1500 rpm with a 1 μm filter. The filtrate is removed after the pH measurement with pH indicator rods (pH = 2.5–3). The solid is then washed several times by dispersion in four 5 L beakers with each 3 L of DI water and 10 min of ultrasound. The washing step is repeated 5 times until a pH of the filtrate greater than 4.5 is reached. After drying overnight in an oven at 90 °C, the white agglomerated powder is ground with cutting mills. Finally, the white powder is heated for 24 h at 150 °C in an oven.

Characterization techniques

This section describes techniques used to characterize the various samples through powder X-ray diffraction (XRD), thermal gravimetric analysis (TGA), N_2 adsorption–desorption, scanning electron microscopy (SEM) and water adsorption capacities.

X-Ray diffraction patterns were collected using a PANalytical MPD X'Pert Pro diffractometer operating in reflection mode with Cu Kα radiation (Kα = 0.15418 nm) and equipped with a PIXcel real-time multiple strip detector (active length = 3.347° (2θ)) and a Bragg Brentano geometry. The powder patterns were collected at ambient temperature in the range of $3 < 2\theta < 50°$, a step of 0.013° (2θ), and a time per step of 220 s. Approximately 400 mg of the sample were finely ground before analysis and placed in a back loading sample holder (stainless steel).

TGA was performed using a TGA/DSC Mettler Toledo apparatus under air flow between 30 and 900 °C in a 70 μL alumina crucible with a heating speed of 2 °C min^{-1}.

The N_2 adsorption–desorption isotherms were realized using an ASAP 2420 Micromeritics analyser at −196 °C. Prior to the sorption measurement, the samples (50–100 mg) were outgassed 12 h at 200 °C under vacuum to remove any gas or vapor from the pores. Microporous volumes ($V_{t\text{-plot}}$) were evaluated with the *t*-plot method. Surface areas were calculated by Brunauer–Emmett–Teller (S_{BET}) and Langmuir (S_{Lang}) methods after applying the criteria recommended by Rouquerol (relative pressure range selected: approximately 0.002–0.04 for p/p^0).[49] The external surface (S_{ext}) was calculated from *t*-plot method.

The morphology of particles from samples and coated by carbonwas studied using a JEOL scanning electron microscope (model JSM 7900F).

Water adsorption capacities were measured at 79% RH and 20 °C using a desiccator with a saturated solution of NH_4Cl.[50]

Results and discussion

The different samples of MOF A520 were synthesized by the hydrothermal method following four different protocols. The impacts of synthesis parameters such as the molar ratio,

temperature, duration and pH on the physico-chemical properties of MOF A520 material are discussed below.

MOF A520 samples prepared from aluminium hydroxide (protocol 1)

Through protocol 1, the impact of the base amount and related pH on the MOF A520 synthesis is discussed. Table 4 reports the composition expressed in molar ratios, the pH measured in the relevant syntheses and the crystallographic phases identified in the samples. The results are described and commented according to the number of NaOH molar equivalent.

Synthesis carried out with 3 molar equivalents of NaOH allows all of the $Al(OH)_3$ (gibbsite) to be dissolved in 1 hour of reflux. However, the pH of the solution formed after the addition of fumaric acid is very basic (pH = 14), not making the formation of MOF A520 possible (required pH = 2–3). The X-ray pattern of sample 1 (Fig. 2, red curve) reveals no characteristic peak of MOF A520 but instead the presence of 4 phases: aluminium hydroxide in three crystalline forms (gibbsite, bayerite, and nordstrandite) obtained by precipitation of aluminium during cooling of the solution after synthesis and sodium fumarate formed by precipitation of fumaric acid in the presence of excess sodium hydroxide.

However, the addition of 2 molar equivalents of NaOH does not make possible the complete dissolution of $Al(OH)_3$ after 2.5 h of heating (cloudy solution). Moreover, the too low acidity of the solution after the addition of fumaric acid (pH = 6) hinders the formation of MOF A520. The X-ray pattern of sample 3 (Fig. 2, purple curve) indicates the presence of 2 phases: the unreacted gibbsite (starting reagent) and the pseudo-bohemite corresponding to the beginning of the crystallization of bohemite with very broad peaks offset from well-crystallized bohemite. No trace of XRD diffraction peaks attributed to crystallized MOF A520 is observed.

Likewise, with 1 molar equivalent of NaOH, all $Al(OH)_3$ are not dissolved despite 3.5 h of heating (opaque solution). However, the pH of the solution after the addition of fumaric acid is acidic (3.5) and corresponds to the pH usually observed during the synthesis of MOF A520 with aluminium sulfate (pH = 2–3). Thus, the X-ray pattern of sample 2 (Fig. 2, green curve) reveals the formation of MOF A520 but also the presence of gibbsite (starting reagent) which has not been fully dissolved. This impurity is not eliminated during washing, due to the very

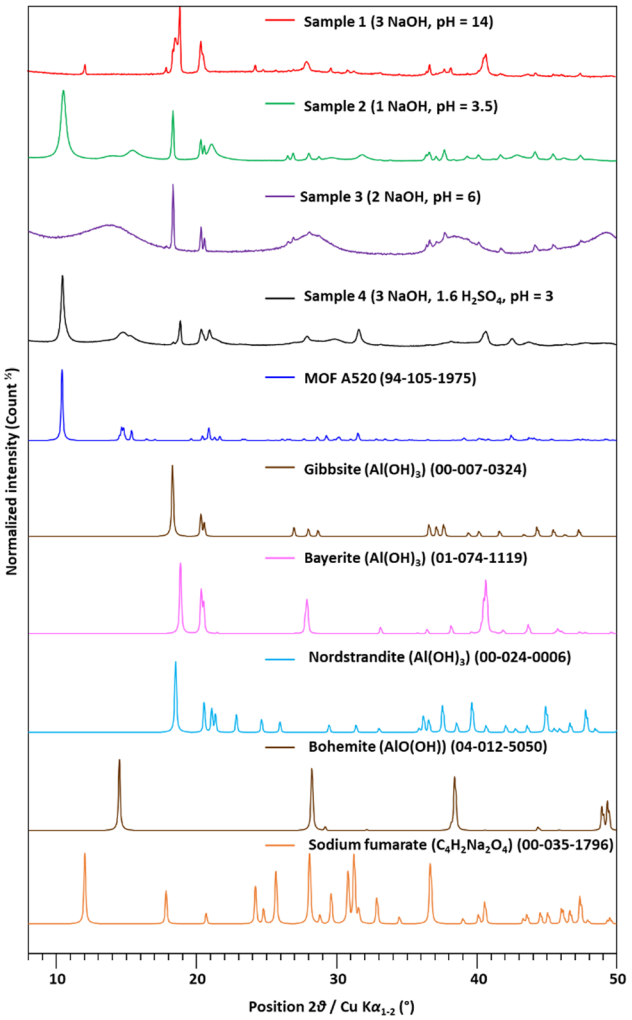

Fig. 2 XRD patterns at wide 2θ angles (Cu Kα radiation) of sample 1 (red), sample 2 (green), sample 3 (purple), sample 4 (black) and patterns of simulated identified phases.

Table 4 Experimental conditions for MOF A520 synthesis from aluminium hydroxide according to protocols 3: molar ratios, pH and identified crystallographic phases

	Molar ratios	pH measured[a]	Identified crystallographic phases[b]
Sample 1	1 $Al(OH)_3$: 1 $C_4H_4O_4$: 3 NaOH : 175 H_2O	14	Gibbsite Bayerite Nordstrandite Sodium fumarate
Sample 3	1 $Al(OH)_3$: 1 $C_4H_4O_4$: 2 NaOH : 175 H_2O	6	Gibbsite Pseudo-bohemite
Sample 2	1 $Al(OH)_3$: 1 $C_4H_4O_4$: 1 NaOH : 175 H_2O	3.5	MOF A520 Gibbsite
Sample 4	1 $Al(OH)_3$: 1 $C_4H_4O_4$: 3 NaOH : 1.6 H_2SO_4 : 175 H_2O	3	Gibbsite MOF A520 Bayerite

[a] pH measurements after mixing all reagents were performed with pH indicator rods. [b] Crystallographic phases were identified with the International Centre for Diffraction Data (ICDD).

low solubility of gibbsite in DI water at room temperature ($K_s = 10^{-34}$ at 25 °C).[51,52]

In this way, only 3 molar equivalents of NaOH make it possible the complete dissolution of $Al(OH)_3$ but the pH has been adjusted to 3 after the addition of fumaric acid to obtain an acidic solution, conducive to the formation of MOF A520. Thus, the addition of 1.6 molar equivalents of sulfuric acid makes it possible to neutralize the excess sodium hydroxide. The X-ray pattern of sample 4 (Fig. 2, black curve) reveals the formation of MOF A520. However, two impurity phases of aluminium hydroxide (gibbsite and bayerite) are obtained, indicating the precipitation of aluminium when changing from a very basic (14) to an acidic pH (3) upon the addition of sulfuric acid.

The experimental conditions evaluated show that the MOF A520 can be synthesized from $Al(OH)_3$ if the pH of the reaction medium is close to 3. However, MOF A520 is not obtained in the form of a single pure crystalline phase, indeed some unreacted aluminium hydroxide remain in the synthesis material.

MOF A520 samples prepared from sodium aluminate (protocol 2)

Through the properties of samples elaborated according to protocol 2, the influence of sodium aluminate as the aluminium precursor for the synthesis of MOF A520 is discussed. Sodium aluminate affords the great advantage of being 3 times cheaper than aluminium sulfate octadecahydrate and can substitute NaOH because of its intrinsic basicity.

Table 5 reports the composition expressed in molar ratios, the pH measured in the relevant syntheses and the phases identified in the samples. During the synthesis of sample 5, involving sodium aluminate, a slightly acidic solution is obtained after mixing sodium aluminate and fumaric acid (pH = 6). Under these conditions, the obtained synthesis material is composed of MOF A520, bayerite and an undefined amorphous phase (Fig. 3, red curve). Thus, to obtain a pure phase of MOF A520, the pH of the solution was adjusted to 3 (the optimal pH defined using protocol 1), with 96% sulfuric acid (sample 6) or 37% hydrochloric acid (sample 7). In this way, pure crystalline phases are obtained (samples 6 and 7, Fig. 3, green curve and purple curve, respectively).

Table 6 summarizes the experimental results related to thermograms, N_2 physisorption, SEM and water adsorption analyses carried out on samples 6 and 7. These two MOF A520 materials were obtained with high yields (82% for sample 6 and 79% for sample 7), without any excess of fumaric acid in the reaction medium, in contrast to the protocol described by Wamba *et al.*[28] (molar ratio: 1 $NaAlO_2$/1.7 fumaric acid to counterbalance the basic pH imposed by the presence of this precursor), thus limiting the loss of reagents. The nanocrystals obtained in both cases are highly agglomerated (Fig. 4(a)), as already reported in the literature (with a size distribution between 60 and 100 nm[17]). The nanosized crystals are the cause of the broadening of the XRD peaks as shown in Fig. 3. During the TGA analysis (Fig. 4(c)), a first weight loss occurs from 25 to 150 °C (3.4% for sample 6 and 4.2% for sample 7) and corresponds to the vaporization of physisorbed water molecules trapped by samples before the analysis. The second weight loss between 150 and 350 °C (2.1% for sample 6 and 3.4% for sample 7) is assigned to the release of unreacted fumaric acid. Finally, the third weight loss concerns the decomposition of the MOF organic linker. This third weight loss is lower than expected (60.5% for sample 6, 55.1% for sample 7

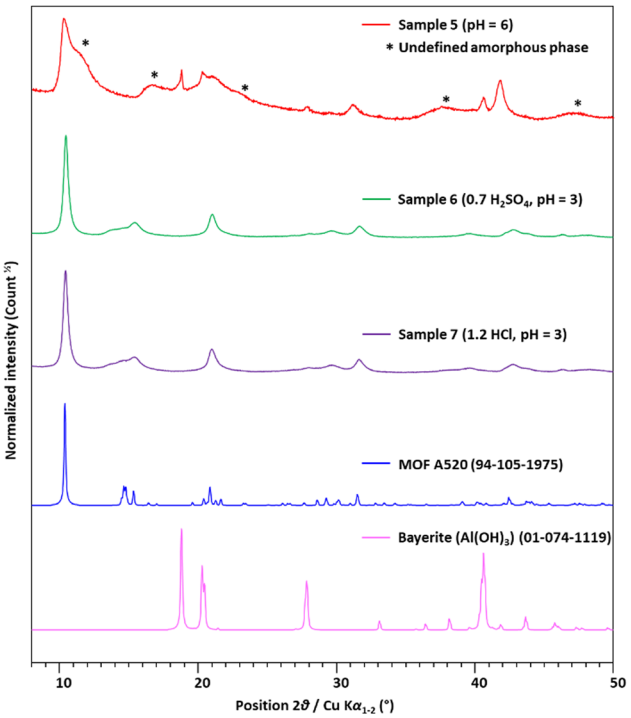

Fig. 3 XRD patterns at wide 2θ angles (Cu Kα radiation) of sample 5 (red), sample 6 (green), sample 7 (purple) and patterns of simulated identified phases.

Table 5 Experimental conditions for MOF A520 synthesis from sodium aluminate according to protocol 2: molar ratios, pH and identified crystallographic phases

	Molar ratios	pH measured[a]	Identified crystallographic phases[b]
Sample 5	1 $NaAlO_2$: 1 $C_4H_4O_4$: 175 H_2O	6	MOF A520, Bayerite Amorphous phase
Sample 6	1 $NaAlO_2$: 1 $C_4H_4O_4$: 0.7 H_2SO_4 : 175 H_2O	3	MOF A520
Sample 7	1 $NaAlO_2$: 1 $C_4H_4O_4$: 1.2 HCl : 179 H_2O	3	MOF A520

[a] pH measurements after mixing all reagents were performed with pH indicator rods. [b] Crystallographic phases were identified with the International Centre for Diffraction Data (ICDD).

Table 6 Textural and physico-chemical properties of MOF A520 synthesis from sodium aluminate according to protocol 2

	Yield (%) (weight, g)	Weight losses[a] (%) 30–150 °C	150–350 °C	350–800 °C	Water uptake[b] (wt%)	Textural properties[c] S_{BET} ($m^2\ g^{-1}$)	S_{Lang} ($m^2\ g^{-1}$)	S_{ext} ($m^2\ g^{-1}$)	$V_{t\text{-plot}}$ ($cm^3\ g^{-1}$)	Average crystal size[d] (nm)
Sample 6	82 (28.8 g)	3.4 ± 0.5	2.1 ± 0.5	60.5 ± 0.5	42.8 ± 0.6	996 ± 1	1041 ± 6	58 ± 1	0.36 ± 0.01	52 ± 17
Sample 7	79 (27.9 g)	4.2 ± 0.5	3.4 ± 0.5	55.1 ± 0.5	43.0 ± 0.6	905 ± 1	964 ± 4	103 ± 1	0.31 ± 0.01	70 ± 20

[a] Weight losses were deduced from TGA (TGA/DSC Mettler Toledo) under air flow. [b] Water adsorption capacities were measured at 79% RH and 20 °C using a desiccator with a saturated solution of NH_4Cl. [c] Textural properties were deduced from N_2 sorption measurements at −196 °C with an ASAP 2420 micromeritics analyser. [d] Average crystal sizes were calculated by measuring 50 crystals from images obtained with JSM 7900F SEM.

and 67.7% for the calculated theoretical value corresponding to the transformation of MOF A520 into alumina). This could reflect the presence of amorphous aluminium-based species into the raw material and would explain the lower microporous volumes for these two samples (Fig. 4(d) and Table 6) in comparison to the values reported in the literature (microporous volume from 0.37 $cm^3\ g^{-1}$ to 0.44 $cm^3\ g^{-1}$ (ref. 1, 17)). Due to their lower microporous volume, the samples show a slightly drop in water adsorption capacity (42.8 wt% for sample 6 and 43.0 wt% for sample 7) compared to the values reported in the literature (44 to 47 wt% at 80% RH by the volumetric method at 25 °C[13,17]). Despite this, the amount of water adsorbed by MOF A520 synthesized from sodium aluminate remains significantly higher than that of LTA type zeolites (21 to 25 wt% at 25 °C[42,46,47]), materials widely used on an industrial scale as moisture scavengers.

MOF A520 samples prepared from aluminium sulfate octadecahydrate with NaOH or KOH bases (protocol 3)

Aluminium sulfate octadecahydrate is commonly used as the precursor for the synthesis of MOF A520. When it is involved in the synthesis protocol, NaOH must be added into the reaction medium for the linker deprotonation, whereas it is not required with sodium aluminate which has the basic properties is chosen as the precursor. By modulating the base amount added, the morphology of MOF A520 particles can be controlled. Table 7 reports the composition expressed in molar ratios, the pH measured in the relevant syntheses and the identified crystallographic phases in the samples. The results of characterization techniques regarding the concerned syntheses are presented in Table 8, Fig. 5 and 6.

During this experimental work, it turned out that the molar base ratios (KOH/Al or NaOH/Al) less than 2 (0.1 to 1) do not make possible the complete dissolution of fumaric acid. Indeed, the pH of these syntheses after the addition of all the reagents is 1 instead of 2.5–3 when the molar composition described by Karmakar *et al.*[24] is applied (2 molar base ratio). Moreover, the reaction yield increases with the molar base ratio, due to a better dissolution (linker deprotonation) of fumaric acid, while the size of the MOF A520 crystals decreases, leading to broadening peaks in X-ray patterns. For example, the

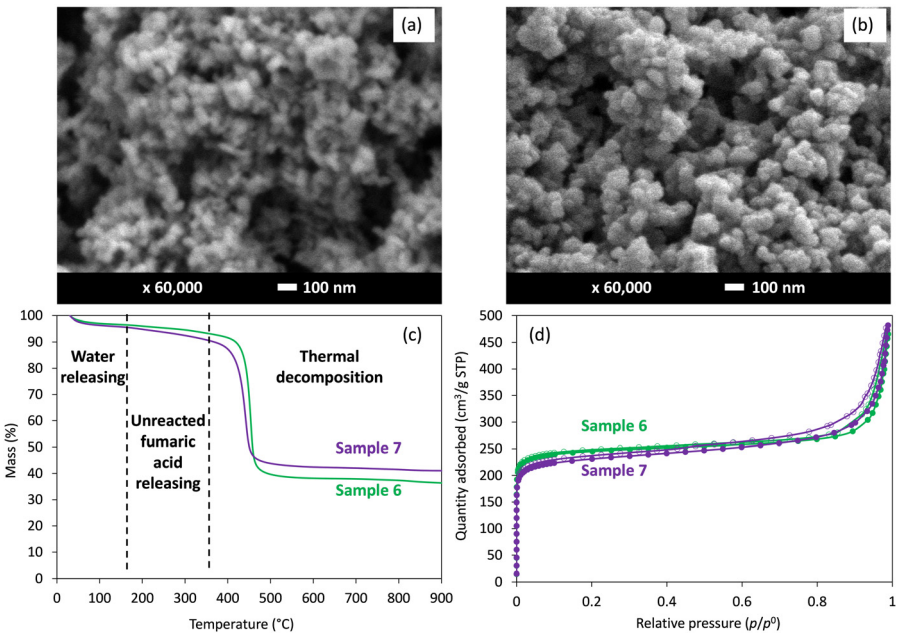

Fig. 4 (a) SEM images of sample 6 and (b) sample 7. (c) Thermogramms under air of sample 6 (green curve) and sample 7 (purple curve). (d) Nitrogen adsorption–desorption isotherms at −196 °C for sample 6 (green curve) and sample 7 (purple curve) (filled and open symbols represent adsorption and desorption isotherms, respectively).

Table 7 Experimental conditions for MOF A520 synthesis from aluminium sulfate octadecahydrate according to protocols 3: molar ratios, duration, temperature, pH and identified crystallographic phases

	Molar ratios	Duration	Temperature (°C)	pH measured[a]	Identified crystallographic phases[b]
Sample 8	1 $Al_2(SO_4)_3{\cdot}18H_2O$: 1 $C_4H_4O_4$: 0.1 KOH : 78 H_2O	13 h 30	100	1	MOF A520
Sample 9	1 $Al_2(SO_4)_3{\cdot}18H_2O$: 1 $C_4H_4O_4$: 0.1 KOH : 78 H_2O	42 h 30	100	1	MOF A520
Sample 10	1 $Al_2(SO_4)_3{\cdot}18H_2O$: 1 $C_4H_4O_4$: 0.1 NaOH : 78 H_2O	44 h 15	100	1	MOF A520
Sample 11	1 $Al_2(SO_4)_3{\cdot}18H_2O$: 1 $C_4H_4O_4$: 0.5 KOH : 78 H_2O	14 h 30	100	1	MOF A520
Sample 12	1 $Al_2(SO_4)_3{\cdot}18H_2O$: 1 $C_4H_4O_4$: 0.8 KOH : 78 H_2O	15 h 15	100	1	MOF A520
Sample 13	1 $Al_2(SO_4)_3{\cdot}18H_2O$: 1 $C_4H_4O_4$: 0.8 KOH : 78 H_2O	42 h 30	100	1	MOF A520
Sample 14	1 $Al_2(SO_4)_3{\cdot}18H_2O$: 1 $C_4H_4O_4$: 0.8 KOH : 78 H_2O	71 h 30	100	1	MOF A520 Alunite
Sample 15	1 $Al_2(SO_4)_3{\cdot}18H_2O$: 1 $C_4H_4O_4$: 1 KOH : 78 H_2O	13 h 20	100	1	MOF A520
Sample 16	1 $Al_2(SO_4)_3{\cdot}18H_2O$: 1 $C_4H_4O_4$: 2 KOH : 78 H_2O	13 h 20	100	2.5–3	MOF A520
Sample 17	1 $Al_2(SO_4)_3{\cdot}18H_2O$: 1 $C_4H_4O_4$: 2 KOH : 184 H_2O	2 h	65	2.5–3	MOF A520
Sample 18	1 $Al_2(SO_4)_3{\cdot}18H_2O$: 1 $C_4H_4O_4$: 2 NaOH : 184 H_2O	2 h	65	2.5–3	MOF A520

[a] pH measurements after mixing all reagents were performed with pH indicator rods. [b] Crystallographic phases were identified with the International Centre for Diffraction Data (ICDD).

X-ray pattern of sample 8 (Fig. 5, red curve) shows very narrow peaks, consistent with the micrometric crystal size (around 11 μm) obtained with a molar ratio of KOH/Al = 0.1 and a yield of 7% (Fig. 6 and Table 7). However, with a molar ratio of 20 times higher and a yield of 63%, sample 16 displays nanometric-sized crystals (around 100 nm, Fig. 6), implying broader peaks on the X-ray pattern (Fig. 5, black curve). Thus, by limiting the deprotonation of the organic source and therefore the reaction kinetics, a low base ratio (0.1) allows the formation of micrometer-sized MOF needles (around 11 μm long and 1.5 μm wide for sample 8, Fig. 6). The latter can then be recovered from the reaction medium by simple filtration on the Büchner funnel or could be collected industrially with a spin dryer.

For similar syntheses conditions (0.1 molar base ratio, 100 °C and 42–44 hours of synthesis), no significant difference between the use of NaOH (sample 10) and KOH (sample 9) is observed. On the other hand, with the addition of 2 molar ratios of the base in the reaction mixture (65 °C and 2 h of synthesis), the nanometric particle size and the textural properties are slightly lower with KOH (sample 17) than NaOH (sample 18), without impacting the water adsorption capacity (Table 8).

The synthesis temperature (100 °C or 65 °C) and the water amount used (78 or 184, so the concentration) do not impact significantly the water adsorption capacity of MOF A520 (44.1 wt% for sample 16 (100 °C and H_2O/Al molar ratio = 78) and 45.4 wt% for sample 17 (65 °C and H_2O/Al molar ratio = 184)). This result is coherent with the literature. Indeed, the hydrothermal synthesis of MOF A520 from aluminium sulfate octadecahydrate can be carried out with variable temperatures: 60 °C,[24] 65 °C,[32] 70 °C,[6] 90 °C[17] and 100 °C.[19] In addition, different water molar ratios are used for the synthesis of MOF A520, ranging from very dilute media (H_2O/Al molar ratio = 306[28]) to concentrated media (H_2O/Al molar ratio = 78[19]), without impacting the material properties. This MOF can also be formed in the total absence of water by grinding the reactants in a twin-screw extruder at 150 °C by three successive passings. This mechanochemical synthesis allows the production of MOF A520 without impacting its crystallinity or porosity (S_{BET} = 1010 $m^2\ g^{-1}$). Nevertheless, water must still be used

Table 8 Textural and physico-chemical properties of MOF A520 synthesis from aluminium sulfate octadecahydrate with NaOH or KOH according to protocols 3

	Yield (%) (weight, g)	Water uptake[a] (wt%)	Textural properties[b]				Average crystal size[c] (nm)
			S_{BET} ($m^2\ g^{-1}$)	S_{Lang} ($m^2\ g^{-1}$)	S_{ext} ($m^2\ g^{-1}$)	$V_{t\text{-plot}}$ ($cm^3\ g^{-1}$)	
Sample 8	7 (0.9 g)	42.6 ± 0.6	1056 ± 1	1090 ± 5	12 ± 1	0.41 ± 0.01	10 996 ± 1308
Sample 9	9 (1.1 g)	43.3 ± 0.6	1039 ± 1	1080 ± 4	11 ± 1	0.41 ± 0.01	18 462 ± 3139
Sample 10	9 (1.1 g)	43.7 ± 0.6	1099 ± 1	1142 ± 4	9 ± 1	0.43 ± 0.01	13 042 ± 2629
Sample 11	18 (2.3 g)	43.7 ± 0.6	1135 ± 1	1186 ± 7	24 ± 1	0.43 ± 0.01	689 ± 370
Sample 12	27 (3.4 g)	43.5 ± 0.6	1116 ± 3	1149 ± 6	29 ± 1	0.43 ± 0.01	388 ± 97
Sample 13	27 (3.4 g)	43.4 ± 0.6	1121 ± 1	1169 ± 6	31 ± 1	0.43 ± 0.01	259 ± 77
Sample 14	— (3.9 g with impurities)	40.8 ± 0.6	1059 ± 1	1103 ± 6	27 ± 1	0.40 ± 0.01	143 ± 44
Sample 15	35 (4.5 g)	44.0 ± 0.6	1135 ± 2	1186 ± 7	69 ± 1	0.42 ± 0.01	113 ± 32
Sample 16	63 (7.9 g)	44.1 ± 0.6	1115 ± 1	1165 ± 6	54 ± 1	0.41 ± 0.01	100 ± 30
Sample 17	71 (25.0 g)	45.4 ± 0.6	1000 ± 3	1044 ± 6	18 ± 1	0.37 ± 0.01	43 ± 17
Sample 18	67 (23.6 g)	46.0 ± 0.6	1127 ± 2	1163 ± 5	76 ± 1	0.41 ± 0.01	81 ± 29

[a] Water adsorption capacities were measured at a 79% RH and 20 °C using a desiccator with a saturated solution of NH_4Cl. [b] Textural properties were deduced from N_2 sorption measurements at −196 °C with an ASAP 2420 micromeritics analyser. [c] Average crystal sizes were calculated by measuring 50 crystals from images obtained with JSM 7900F SEM.

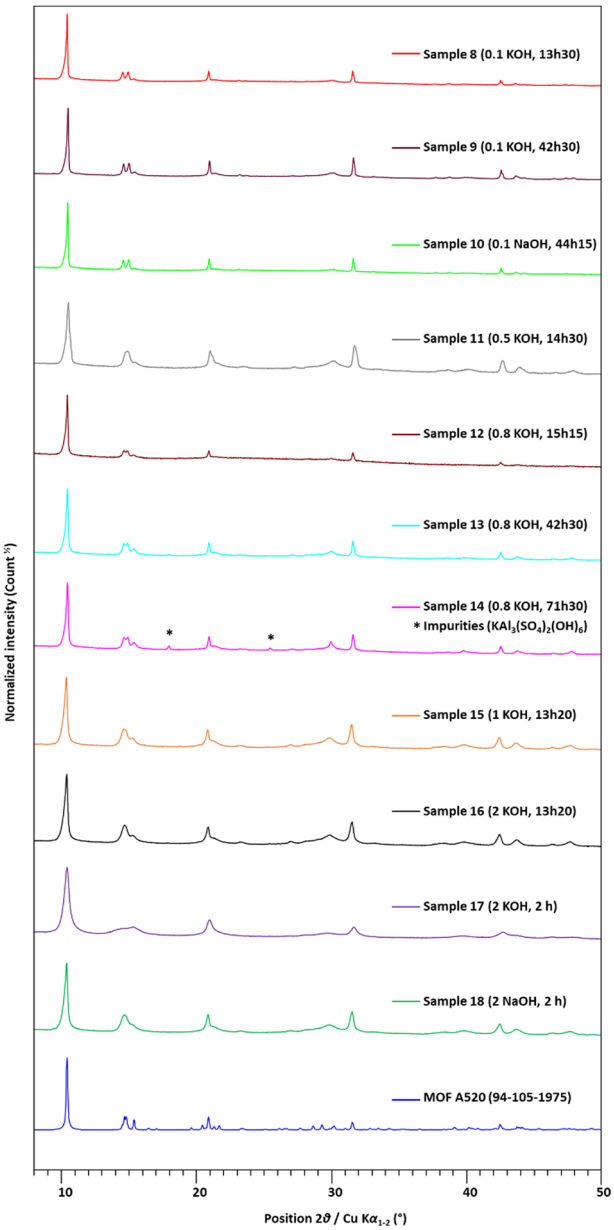

Fig. 5 XRD patterns at wide 2θ angles (Cu Kα radiation) of MOF A520 synthesized from aluminium sulfate octadecahydrate with NaOH or KOH and the pattern of simulated MOF A520.

subsequently to wash the material and eliminate the by-product Na_2SO_4.[33] However, at 65 °C and with a H_2O/Al molar ratio of 184 (sample 17), the average crystal size and the pore volume are smaller than at 100 °C and with a H_2O/Al molar ratio of 78 (sample 16) (43 nm and 0.37 $cm^3\ g^{-1}$, 100 nm and 0.41 $cm^3\ g^{-1}$, respectively) (Table 8). It is worth noting that the synthesis duration is 6.6 times longer for the synthesis of sample 16 than for the synthesis of sample 17 that may explains the differences in textural properties and morphology than the temperature or concentration of reaction mixtures. Thus, the synthesis temperature proposed by Li *et al.*[19] (100 °C) can be lowered to 65 °C without significant modification of the MOF A520 properties, allowing energy saving and therefore cost reduction.

The synthesis duration impacts to a lesser extent the yield but mostly the size of the crystals. For a molar ratio of 0.1 KOH, increasing the synthesis duration from 13 h 30 (sample 8) to 42 h 30 (sample 9) increases the particle size (approximately from 11 to 18 μm, respectively) but slightly the yields (7 and 9%, respectively) (Table 8). Besides, for a ratio of 0.8 KOH, increasing the synthesis time from 15 h 15 (sample 12) to 42 h 30 (sample 13) and 71 h 30 (sample 14) implies a gradual reduction in the particle size (around 388 nm, 259 nm and 143 nm, respectively), probably due to a partial redissolution of crystals over time. Furthermore, after 71 h 30 of synthesis using a 0.8 molar ratio of KOH (sample 14), a second phase appears (Fig. 5, pink curve). This phase is identified as alunite ($KAl_3(SO_4)_2(OH)_6$) which is not soluble in water but in sulfuric acid and therefore not eliminated during the washing step.[53,54]

The textural properties of MOF A520 are slightly affected by the nature of the base used, its molar ratio and the synthesis time/temperature in this system (Table 8). However, the water adsorption capacity (approximately 42–43 wt%) is slightly lower than expected (44 to 47 wt% at an 80% RH by the volumetric method at 25 °C[13,17]) for base/Al molar ratios below 1. This may be due to a lower contribution of inter-particle mesoporosity and the number of hydrophilic sites on the external surface of MOF A520 particles. Indeed, the external surfaces measured in a nitrogen adsorption decrease when the base concentration decreases (from 31 to 9 $m^2\ g^{-1}$). For sample 14, the water adsorption value is particularly low (40.8 wt%). This is due to alunite impurity, which can only adsorb between 5 and 16 wt% water at an 80% RH and 30 °C,[55] thus reducing the apparent capacity of the MOF A520/alunite mixture. Despite this drop in capacity, the quantity of water adsorbed by MOF A520 remains significantly higher than that of LTA type zeolites.

For industrial scale production, high yields are required. The MOF A520 synthesis from aluminium sulfate octadecahydrate with 2 molar equivalents of NaOH and 2 h of synthesis at 65 °C (sample 18, yield = 63%) therefore remains the best solution despite a nanometric crystal size grouped into micrometer sized agglomerates (Fig. 6).

Scale-ups of the MOF A520 synthesis from aluminium sulfate octadecahydrate (protocol 4)

Thanks to the 10-factor scaled-up preparation, 230 g of MOF A520 were obtained per batch that being 2.3 kg of MOF A520 with the nine repetitions of the synthesis. The second scale-up with a factor of 100 allowed to obtain 2.3 kg of MOF A520 per batch.

These MOF A520 samples obtained on a large scale show similar textural (S_{BET}, S_{Lang} $V_{t\text{-plot}}$, S_{ext}), structural and morphological (nanoparticles) properties than their counterparts obtained in 1 L bottles. Indeed, MOF A520 was identified in each X-ray pattern as the only phase whatever the synthesis scale, without crystalline impurity (Fig. 7). In addition, the broadening peaks in X-ray patterns reflect a nanometric size of the MOF crystals, proven by scanning electron microscopy. The crystal sizes decrease with the scale-up of the syntheses, from around 81 nm on the laboratory scale to around 44 nm for the 100-factor scale-up (Table 9).

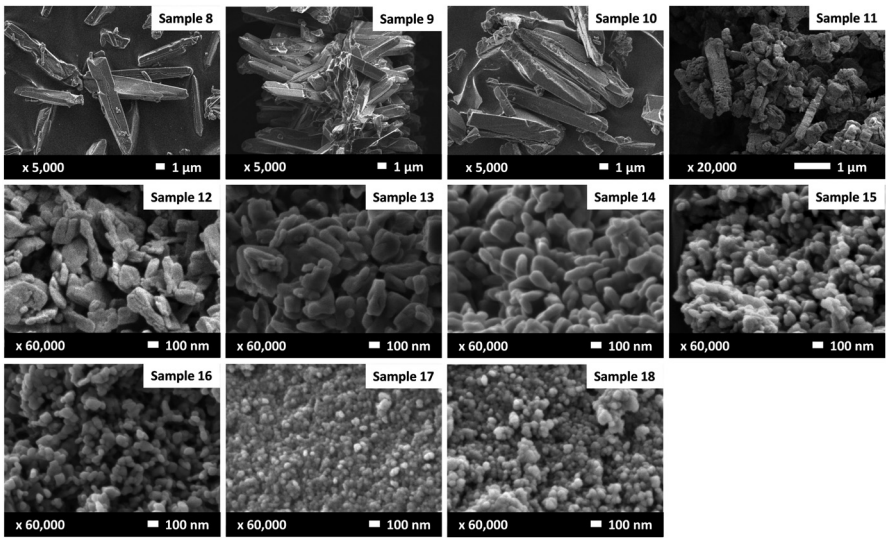

Fig. 6 SEM images of MOF A520 synthesized according to protocols 3.

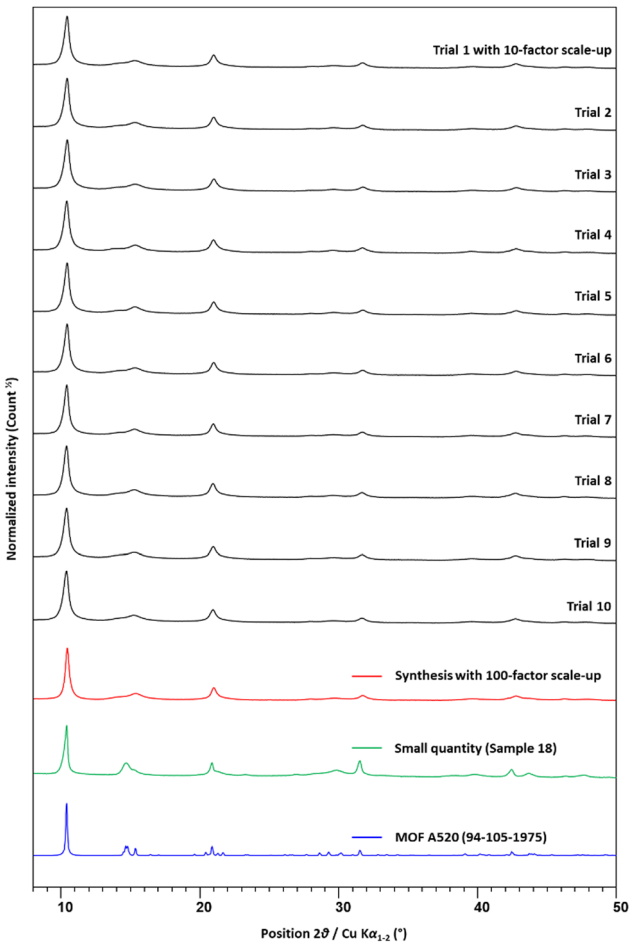

Fig. 7 XRD patterns at wide 2θ angles (Cu Kα radiation) of MOF A520 synthesized from aluminium sulfate octadecahydrate with NaOH for the ten syntheses of the 10-factor scale-up (black curves), the 100-factor scale-up (red curve) and the laboratory scale (green curve). The pattern of simulated MOF A520 (blue curve).

Moreover, scaling does not seem to impact the textural properties of MOF A520, and the values obtained are coherent with the literature (microporous volume from 0.37 $cm^3\ g^{-1}$ to 0.44 $cm^3\ g^{-1}$ (ref. 1, 17)).

However, the water adsorption capacity for the 100-factor scale-up sample is slightly lower (42.8 $\pm$ 0.6 wt%) than expected (45.2 to 46 $\pm$ 0.6 wt% at an 80% RH by the volumetric method at 25 °C[13,17]). This was attributed to the presence of gibbsite in the sample, too low to be detected by XRD (<5%) but sufficient to impact the product performance. This was the consequence of a long filtration/washing step and storage of the obtained solution. A faster and adapted filtration process will help to overcome this problem and obtain a pure MOF A520 on the kilogram or ton scale.

Despite, the quantity of water adsorbed by MOF A520 remains significantly higher than that of LTA type zeolites. These different results confirm that the synthesis of MOF A520 from aluminium sulfate octadecahydrate is reproducible on a large scale. This confirmation and the synthesis optimization results presented in this paper allow us to foresee the production of MOF A520 on a ton scale thanks to an industrial partner but this time from sodium aluminate (reduced cost and better yield).

Conclusions

APTAR CSP Technologies has marked our society with its highly adapted solutions for protection against moisture that are supplied worldwide. In the continuous improvement process, the optimization of their technologies (by increasing its scavenging capacity) is a priority. These findings shed light on the optimal conditions for the low cost green production of MOF A520 and its high potential as an efficient humidity scavenger in comparison to 3A or 4A zeolites, the most used industrial humidity scavengers. MOF A520 as a desiccant will advantageously substitute zeolites in 3 phase active polymer™ formulations patented by APTAR CSP Technologies. This technology

Table 9 Textural and physico-chemical properties of MOF A520 synthesis from aluminium sulfate octadecahydrate with NaOH according to protocol 4

	Water uptake[a] (wt%)	Textural properties[b]				Average crystal size[c] (nm)
		S_{BET} ($m^2\ g^{-1}$)	S_{Lang} ($m^2\ g^{-1}$)	S_{ext} ($m^2\ g^{-1}$)	$V_{t\text{-plot}}$ ($cm^3\ g^{-1}$)	
10-Factor scaled-up synthesis	45.2 ± 0.6	1094 ± 2	1152 ± 5	86 ± 1	0.39 ± 0.01	63 ± 25
100-Factor scaled-up synthesis	42.8 ± 0.6	1061 ± 1	1097 ± 5	32 ± 1	0.40 ± 0.01	44 ± 10
Small quantity (sample 18)	46.0 ± 0.6	1127 ± 2	1097 ± 5	76 ± 1	0.41 ± 0.01	81 ± 29

[a] Water adsorption capacities were measured at a 79% RH and 20 °C using a desiccator with a saturated solution of NH_4Cl. [b] Textural properties were deduced from N_2 sorption measurements at −196 °C with an ASAP 2420 micromeritics analyser. [c] Average crystal sizes were calculated by measuring 50 crystals from images obtained with JSM 7900F SEM.

allows us to control humidity within the active packaging and improve the preservation of pharmaceutical products which are sensitive to humidity, thus reducing their degradation while guaranteeing patient safety.

Through the application of several protocols, we explored the impact of different parameters on the hydrothermal synthesis of MOF A520 such as the aluminium precursor, the nature and ratios of the bases, and the reaction conditions (duration, temperature, and concentration). The crucial parameter for the formation of pure MOF A520 is the pH of the reaction medium. The latter should ideally be around 3. At pH = 1, fumaric acid does not dissolve completely whereas at pH superior to 6, the MOF A520 does not crystallize.

The use of aluminium hydroxide as an aluminium precursor does not allow the formation of MOF A520 without the presence of crystalline impurities, due to incomplete dissolution of the aluminium source. On the other hand, sodium aluminate is suitable for the synthesis of MOF A520 under stoichiometric conditions combined with the addition of acid (sulfuric or hydrochloric) to compensate the basicity of the aluminate. The MOF A520 samples thus obtained display a slightly lower water adsorption capacity (42–43 wt%) compared to the samples synthesized from aluminium sulfate octadecahydrate (44–46 wt%) but with better yields (79–82% *versus* 7–71%, respectively). Moreover, it is worth noting that when MOF A520 is synthesized from sodium aluminate or aluminium sulfate octadecahydrate, its water adsorption capacities are greater than those of 3A and 4A zeolites (21 to 25 wt%). The MOF A520 synthesis from sodium aluminate therefore appears to be an optimal solution for producing this material from a sustainable point of view (higher yields, reduced costs, non-toxic reagents and solvents). Indeed, sodium aluminate is three times cheaper than aluminium sulfate octadecahydrate and allows the production of MOF A520 with a higher yield (+10%) thus limiting losses. The reduction in its effectiveness as a desiccant is negligible (−3%) compared to the advantages obtained through the modification of the metal precursor.

Additionally, using aluminium sulfate octadecahydrate as the aluminium source, micrometer-sized crystals (around 10 μm needles) can be obtained by reducing the molar base ratio (KOH or NaOH) to 0.1 instead of 2, allowing easier MOF A520 recovery on an industrial scale. But the yield is affected (7% after 13 h 30 of synthesis at 100 °C *versus* 67% after 2 h of synthesis at 65 °C and crystals smaller than 100 nm). A compromise must therefore be made between the particle size and the synthesis yield, depending on the targeted applications. Moreover, the MOF A520 synthesis from aluminium sulfate octadecahydrate can be achieved on a kilogram scale without significant loss of performance. Under these conditions, the optimized parameters are 2 h of synthesis at 65 °C with 2 molar equivalents of NaOH.

Thanks to its hydrothermal synthesis which can be carried out on a large scale and the use of non-toxic reagents for human health (especially fumaric acid which is used as an additive in the food industry), MOF A520 can be an alternative to LTA type zeolites as moisture scavengers due to its almost twice higher water adsorption capacity.

Data availability

All relevant data supporting this article have been included in the manuscript and data will be made available upon request.

Conflicts of interest

There are no conflicts to declare.

Acknowledgements

The authors thank the French National Association for Research and Technology (ANRT) and Aptar CSP Technologies for financial support (2022/0721). The authors also thank the technical platforms of IS2M where XRD analyses, nitrogen sorption measurements, recordings by scanning electronic microscopy and thermogravimetric analyses were performed.

References

1 E. Alvarez, N. Guillou, C. Martineau, B. Bueken, B. Van de Voorde, C. Le Guillouzer, P. Fabry, F. Nouar, F. Taulelle, D. de Vos, J. S. Chang, K. H. Cho, N. Ramsahye, T. Devic, M. Daturi, G. Maurin and C. Serre, *Angew. Chem., Int. Ed.*, 2015, **54**, 3664–3668.
2 J. A. Coelho, A. E. O. Lima, A. E. Rodrigues, D. C. S. de Azevedo and S. M. P. Lucena, *Adsorption*, 2017, **23**, 423–431.
3 Z. L. Guo, N. Wu, Y. Wu, C. X. Sun, H. L. Wu and Q. Li, *Microporous Mesoporous Mater.*, 2022, **343**, 112168.
4 B. Han and A. Chakraborty, *Microporous Mesoporous Mater.*, 2019, **288**, 109590.

5 E. Hasturk, C. Schlusener, J. Quodbach, A. Schmitz and C. Janiak, *Microporous Mesoporous Mater.*, 2019, **280**, 277–287.
6 Z. B. Liu, C. J. Cheng, J. D. Han, X. Qi, Z. Zhao and R. N. Teng, *Appl. Therm. Eng.*, 2021, **199**, 117570.
7 B. Q. Tan, Y. S. Luo, X. H. Liang, S. F. Wang, X. N. Gao, Z. G. Zhang and Y. T. Fang, *Ind. Eng. Chem. Res.*, 2019, **58**, 15712–15720.
8 B. Q. Tan, Y. S. Luo, X. H. Liang, S. F. Wang, X. N. Gao, Z. G. Zhang and Y. T. Fang, *Cryst. Growth Des.*, 2020, **20**, 6565–6572.
9 Q. Liu, Y. Ding, Q. Liao, X. Zhu, H. Wang and J. Yang, *Colloids Surf., A*, 2019, **579**, 123645.
10 L. X. Guo, J. Hurd, M. He, W. P. Lu, J. N. Li, D. Crawshaw, M. T. Fan, S. Sapchenko, Y. L. Chen, X. D. Zeng, M. Kippax-Jones, W. Y. Huang, Z. D. Zhu, P. Manuel, M. D. Frogley, D. Lee, M. Schroder and S. H. Yang, *Commun. Chem.*, 2023, **6**, 55.
11 L. Zhou, X. Zhang and Y. Chen, *Mater. Lett.*, 2017, **197**, 224–227.
12 A. Cadiau, J. S. Lee, D. D. Borges, P. Fabry, T. Devic, M. T. Wharmby, C. Martineau, D. Foucher, F. Taulelle, C. H. Jun, Y. K. Hwang, N. Stock, M. F. De Lange, F. Kapteijn, J. Gascon, G. Maurin, J. S. Chang and C. Serre, *Adv. Mater.*, 2015, **27**, 4775–4780.
13 E. Elsayed, R. Al-Dadah, S. Mahmoud, A. Elsayed and P. A. Anderson, *Appl. Therm. Eng.*, 2016, **99**, 802–812.
14 S. Gokpinar, S. J. Ernst, E. Hasturk, M. Mollers, I. El Aita, R. Wiedey, N. Tannert, S. Niessing, S. Abdpour, A. Schmitz, J. Quodbach, G. Fuldner, S. K. Henninger and C. Janiak, *Ind. Eng. Chem. Res.*, 2019, **58**, 21493–21503.
15 I. Jahan, M. A. Islam, M. L. Palash, K. A. Rocky, T. H. Rupam and B. B. Saha, *Heat Transfer Eng.*, 2021, **42**, 1132–1141.
16 F. Jeremias, D. Fröhlich, C. Janiak and S. K. Henninger, *RSC Adv.*, 2014, **4**, 24073–24082.
17 S. Kayal, A. Chakraborty and H. W. B. Teo, *Mater. Lett.*, 2018, **221**, 165–167.
18 H. Kummer, F. Jeremias, A. Warlo, G. Fuldner, D. Frohlich, C. Janiak, R. Glaser and S. K. Henninger, *Ind. Eng. Chem. Res.*, 2017, **56**, 8393–8398.
19 Q. Q. Li, Y. F. Ying, Y. L. Tao and H. Q. Li, *Ind. Eng. Chem. Res.*, 2022, **61**, 1344–1354.
20 H. W. B. Teo, A. Chakraborty and S. Kayal, *Microporous Mesoporous Mater.*, 2018, **272**, 109–116.
21 H. W. B. Teo, A. Chakraborty, Y. Kitagawa and S. Kayal, *Int. J. Heat Mass Transfer*, 2017, **114**, 621–627.
22 P. G. Yot, L. Vanduyfhuys, E. Alvarez, J. Rodriguez, J. P. Itie, P. Fabry, N. Guillou, T. Devic, I. Beurroies, P. L. Llewellyn, V. Van Speybroeck, C. Serre and G. Maurin, *Chem. Sci.*, 2016, **7**, 446–450.
23 S. Karmakar, S. Bhattacharjee and S. De, *J. Environ. Chem. Eng.*, 2017, **5**, 6087–6097.
24 S. Karmakar, J. Dechnik, C. Janiak and S. De, *J. Hazard. Mater.*, 2016, **303**, 10–20.
25 E. Moumen, L. Bazzi and S. E. Hankari, *Process Saf. Environ. Prot.*, 2022, **160**, 502–512.
26 Z. H. Huang, P. Hu, J. Liu, F. Shen, Y. Q. Zhang, K. A. Chai, Y. P. Ying, C. J. Kang, Z. Q. Zhang and H. B. Ji, *Sep. Purif. Technol.*, 2022, **286**, 120446.
27 M. Rivera-Torrente, D. Kroon, M.-V. Coulet, C. Marquez, N. Nikolopoulos, R. Hardian, S. Bourrelly, D. de Vos, G. Whiting and B. M. Weckhuysen, *Chem. – Eur. J.*, 2022, **28**, e202103420.
28 H. N. Wamba, N. Singh, S. Dalakoti, S. Divekar, A. Arya, A. T. C. Kuate, J. Ngoune and S. Dasgupta, *ChemistrySelect*, 2023, **8**, e202204476.
29 S. Abdi and M. Nasiri, *ACS Appl. Mater. Interfaces*, 2019, **11**, 15060–15070.
30 Y. Wang, Q. T. Qu, G. Liu, V. S. Battaglia and H. H. Zheng, *Nano Energy*, 2017, **39**, 200–210.
31 Y. Khani, N. Kamyar, F. Bahadoran, N. Safari and M. M. Amini, *Renewable Energy*, 2020, **156**, 1055–1064.
32 M. Rubio-Martinez, T. D. Hadley, M. P. Batten, K. Constanti-Carey, T. Barton, D. Marley, A. Monch, K. S. Lim and M. R. Hill, *ChemSusChem*, 2016, **9**, 938–941.
33 D. Crawford, J. Casaban, R. Haydon, N. Giri, T. McNally and S. L. James, *Chem. Sci.*, 2015, **6**, 1645–1649.
34 D. E. Crawford and J. Casaban, *Adv. Mater.*, 2016, **28**, 5747–5754.
35 M. Gaab, N. Trukhan, S. Maurer, R. Gummaraju and U. Muller, *Microporous Mesoporous Mater.*, 2012, **157**, 131–136.
36 D. Mohapatra, S. Mishra, S. Giri and A. Kar, *Trends Post-Harvest Technol.*, 2013, **1**, 37–54.
37 C. B. Watkins and J. F. Nock, *Production guide for storage of organic fruits and vegetables*, Department of Horticulture, Cornell University, 2012.
38 D. R. Burfield, K.-H. Lee and R. H. Smithers, *J. Org. Chem.*, 1977, **42**, 3060–3065.
39 M. Lam, R. F. Louie, C. M. Curtis, W. J. Ferguson, J. H. Vy, A.-T. Truong, S. L. Sumner and G. J. Kost, *J. Diabetes Sci. Technol.*, 2014, **8**, 83–88.
40 O. Mansour, M. Isbera, G. Ismail and G. Mayya, *World J. Pharm. Res.*, 2018, **7**, 35–44.
41 K. C. Waterman and B. C. MacDonald, *J. Pharm. Sci.*, 2010, **99**, 4437–4452.
42 E.-P. Ng and S. Mintova, *Microporous Mesoporous Mater.*, 2008, **114**, 1–26.
43 L. M. Liu, S. L. Tan, T. Horikawa, D. D. Do, D. Nicholson and J. J. Liu, *Adv. Colloid Interface Sci.*, 2017, **250**, 64–78.
44 C. Jia, Y. Dai, J. Wu and R. Wang, *Int. J. Refrig.*, 2007, **30**, 345–353.
45 F. Jeremias, D. Fröhlich, C. Janiak and S. K. Henninger, *New J. Chem.*, 2014, **38**, 1846–1852.
46 Z. Tahraoui, H. Nouali, C. Marichal, P. Forler, J. Klein and T. J. Daou, *Molecules*, 2021, **26**, 4815–4841.
47 M. Tatlier, G. Munz and S. K. Henninger, *Microporous Mesoporous Mater.*, 2018, **264**, 70–75.
48 M. Ghodhbene, F. Bougie, P. Fongarland and M. C. Iliuta, *Can. J. Chem. Eng.*, 2017, **95**, 1842–1849.
49 K. S. Walton and R. Q. Snurr, *J. Am. Chem. Soc.*, 2007, **129**, 8552–8556.

50 L. Greenspan, *J. Res. Natl. Bur. Stand., Sect. A*, 1977, **81**, 89–96.
51 B. Fritz and Y. Tardy, *Sci. Geol., Bull.*, 1973, **4** 339–367.
52 B. Sanjuan and G. Michard, *Bull. Mineral.*, 1987, **110**, 567–577.
53 J. A. Ripmeester, C. I. Ratcliffe, J. E. Dutrizac and J. L. Jambor, *Can. Mineral.*, 1986, **24**, 435–447.
54 R. Stoffregen, C. N. Alpers and J. L. Jambor, *Rev. Mineral. Geochem.*, 2000, **40**, 453–479.
55 M. Kurata, K. Kaneko and K. Inouye, *J. Phys. Chem.*, 1984, **88**, 2119–2124.

